Integrase-Deficient Lentiviral Vectors Mediate Efficient Gene Transfer to Human Vascular Smooth Muscle Cells with Minimal Genotoxic Risk

Helen E. Chick,[1] Ali Nowrouzi,[2] Raffaele Fronza,[2] Robert A. McDonald,[1] Nicole M. Kane,[1,3] Raul Alba,[1] Christian Delles,[1] William C. Sessa,[4] Manfred Schmidt,[2] Adrian J. Thrasher,[3] Andrew H. Baker[1]

Abstract

We have previously shown that injury-induced neointima formation was rescued by adenoviral-Nogo-B gene delivery. Integrase-competent lentiviral vectors (ICLV) are efficient at gene delivery to vascular cells but present a risk of insertional mutagenesis. Conversely, integrase-deficient lentiviral vectors (IDLV) offer additional benefits through reduced mutagenesis risk, but this has not been evaluated in the context of vascular gene transfer. Here, we have investigated the performance and genetic safety of both counterparts in primary human vascular smooth muscle cells (VSMC) and compared gene transfer efficiency and assessed the genotoxic potential of ICLVs and IDLVs based on their integration frequency and insertional profile in the human genome. Expression of enhanced green fluorescent protein (eGFP) mediated by IDLVs (IDLV-eGFP) demonstrated efficient transgene expression in VSMCs. IDLV gene transfer of Nogo-B mediated efficient overexpression of Nogo-B in VSMCs, leading to phenotypic effects on VSMC migration and proliferation, similar to its ICLV version and unlike its eGFP control and uninfected VSMCs. Large-scale integration site analyses in VSMCs indicated that IDLV-mediated gene transfer gave rise to a very low frequency of genomic integration compared to ICLVs, revealing a close-to-random genomic distribution in VSMCs. This study demonstrates for the first time the potential of IDLVs for safe and efficient vascular gene transfer.

Introduction

Vascular gene delivery strategies have been extensively explored in the context of prevention of neointima formation (NIF) (Rissanen and Yla-Herttuala, 2007; Karvinen and Yla-Herttuala, 2010; Hedman et al., 2011). There is a requirement to identify and provide a safe and effective gene transfer strategy for therapeutic gene delivery to attenuate the NIF in this clinical setting. There are many therapeutic genes that have been reported to modulate vascular smooth muscle cell (VSMC) migration and/or proliferation and successfully prevent in-stent restenosis (ISR) and/or vein graft failure in animal models. These include endothelial nitric oxide synthase (eNOS) (Janssens et al., 1998; Varenne et al., 1998); inducible nitric oxide synthase (iNOS) (Kibbe et al., 2001); tissue

inhibitors of Metalloproteinases 1-3 (TIMPs 1-3) (George et al., 1998a; George et al., 1998b; George et al., 2000; George et al., 2011); p53 (George et al., 2001); and Nogo-B (Acevedo et al., 2004; Kritz et al., 2008). The majority of studies have used adenovirus-mediated gene transfer due to its relative ease of production. Indeed, advances have demonstrated stent-based adenoviral delivery of TIMP-3 (Johnson et al., 2005), and eNOS (Sharif et al., 2008) reduced ISR in vivo. However, the commonly used serotype 5 vectors (Ad5) display a high frequency of neutralizing antibodies in the general population (Abbink et al., 2007; Parker et al., 2009) and relatively poor levels of gene transfer to VSMC, the target cell type of many of the aforementioned strategies. Lack of coxsackie and adenovirus receptor (CAR) on this cell type is purported to be the main reason for low level VSMC gene transfer (Nicklin et al., 2001).

[1]British Heart Foundation Glasgow Cardiovascular Research Centre, Institute of Cardiovascular and Medical Sciences, University of Glasgow, Glasgow G12 8TA, United Kingdom.
[2]Department of Translational Oncology, National Center for Tumor Diseases (NTC) and German Cancer Research Center (DKFZ), 69120 Heidelberg, Germany.
[3]Molecular Immunology Unit, Centre for Immunodeficiency, Institute of Child Health, University College London, London WC1N 1EH, United Kingdom.
[4]Department of Pharmacology, Vascular Biology and Therapeutics, Yale University School of Medicine, New Haven, CT 06520-8066.

Nogo (RTN4)-spliced variants A, B, and C are members of the reticulon superfamily of transmembrane proteins associated primarily with the endoplasmic reticulon (ER) (Oertle and Schwab, 2003; Teng and Tang, 2008). Nogo-B has many biological roles; for example, it acts as a pro-apoptotic protein/tumor suppressor (Tagami et al., 2000; Li et al., 2001; Oertle et al., 2003; Watari and Yutsudo 2003; Tambe et al., 2004; Kuang et al., 2006); plays a role in the acute inflammation response (Di Lorenzo et al., 2010) and in pulmonary hypertension (Munoz and Zorzano 2011; Sutendra et al., 2011); is a regulator in vascular (Acevedo et al., 2004), renal (Marin et al., 2010) and hepatic (Zhang et al., 2011) injuries; and plays roles in inflammation of the asthmatic lung (Wright et al., 2010; Xu et al., 2011) and inflammation and tissue repair in response to ischemia (Yu et al., 2009). Previous studies have documented high levels of Nogo-B in vascular endothelial cells (VECs), VSMCs (Acevedo et al., 2004) and monocytes/macrophages (Paszkowiak et al., 2007; Rodriguez-Feo et al., 2007; Yu et al., 2009).

Endogenous Nogo-B expression is important for vascular maintenance and remodeling (Acevedo et al., 2004), as well as cardiac function (Bullard et al., 2008). Indeed, mice deficient in Nogo-A/B demonstrated accelerated rates of NIF after acute vascular injury, which were attenuated/rescued by adenoviral gene transfer of Nogo-B (Acevedo et al., 2004). Nogo-B expression is down-regulated in human arterial atherosclerotic plaques (Rodriguez-Feo et al., 2007; Lee et al., 2009), stenotic lesions (Rodriguez-Feo et al., 2007), and lesions of aortic aneurysms (Pan et al., 2007), and therefore can be regarded as a biomarker for injury-induced NIF (Paszkowiak et al., 2007). Hence, Nogo-B is a therapeutic candidate gene in the vascular gene therapy setting for the prevention of the NIF following acute vascular injury.

Nogo-B acts as a positive and negative regulator of vascular cells by mediating the chemo-attraction of VECs (Acevedo et al., 2004; Miao et al., 2006; Zhao et al., 2010) and antagonizing the migration (Acevedo et al., 2004; Kritz et al., 2008) and proliferation (Kritz et al., 2008) of VSMCs, respectively. We have previously shown that NIF was rescued in a porcine vein graft model and a wire injured mouse model by adenoviral gene transfer of Nogo-B (Kritz et al., 2008).

In comparison to Ad5-based systems, there are many advantageous characteristics that suggest lentiviral vectors (LV) to be favorable gene delivery vectors for vascular gene transfer. LVs are highly efficient at transducing vascular cells (Dishart et al., 2003; Cefai et al., 2005; Qian et al., 2006; Yang et al., 2010) and have been considered as a useful vector for delivering therapeutic interventions to reduce NIF following acute vascular injury in vivo (Qian et al., 2006; Yang et al., 2010). LVs are integration-competent (ICLV) and integrate a transgene copy into the chromosome of the target cell, which allows for efficient, stable, and long-term transgene expression (Matrai et al., 2010).

In contrast, integration-deficient lentiviral vectors (IDLV) are very attractive gene transfer tools since they maintain the efficiency of gene transfer yet have a reduced frequency of integration (Yanez-Munoz et al., 2006; Wanisch and Yanez-Munoz, 2009). IDLVs mediate transient gene expression in proliferating cells (Nightingale et al., 2006; Philippe et al., 2006; Apolonia et al., 2007; Matrai et al., 2011) and provide stable and efficient transgene expression in nondividing cells (Philippe et al., 2006; Yanez-Munoz et al., 2006; Apolonia

et al., 2007; Rahim et al., 2009; Matrai et al., 2011), with minimal integration frequencies (Yanez-Munoz et al., 2006; Apolonia et al., 2007; Wanisch and Yanez-Munoz 2009; Matrai et al., 2011) associated with a reduced risk of insertional mutagenesis or oncogenesis (Hacein-Bey-Abina et al., 2003a; Hacein-Bey-Abina et al., 2003b; Hacein-Bey-Abina et al., 2008; Howe et al., 2008; Kane et al., 2010).

Additionally, IDLVs offer an alternative yet promising option that would be highly advantageous in vascular cell gene transfer (George et al., 2006; White et al., 2007) associated with a higher safety profile. Large-scale studies denoting the integration pattern and genotoxicity of LVs have shown a substantially reduced frequency of insertional induced alteration of cellular genes compared to gamma-retroviral vectors (Montini et al., 2006; Modlich et al., 2009; Montini et al., 2009; Balaggan et al., 2011). However, an inherent genotoxic risk based on vector design is still present (Nowrouzi et al., 2011). In particular, the interaction of the LV integration machinery with cellular factors may be responsible for the proposed cell type- and species-specific integration pattern of LV-based vectors (Lewinski et al., 2006; Bartholomae et al., 2011; Biasco et al., 2011; Biasco et al., 2012).

Integration-site (IS) analyses of the first clinical trial for treatment of adrenoleukodystrophy (ALD) with LV-based vectors has not revealed any insertional-induced side effects (Cartier et al., 2009). A comparative analysis of IS hotspots has demonstrated a mega base-wide LV integration preference without obvious skewing of oncogene targeting (Biffi et al., 2011). To date, large-scale studies of LV integration patterns were performed in cell lines and primary murine and human cells of the hematopoietic system (Bushman et al., 2005; Nowrouzi et al., 2011). Due to an inserted mutation in the LV integrase gene, the integration of IDLV-based vectors is not driven by the viral integrase but by transient DNA-double strand (DSB) sites in the host genome, with residual integrase activity leading to lower frequency of random integration frequency as compared to ICLVs (Yanez-Munoz et al., 2006; Wanisch and Yanez-Munoz 2009; Matrai et al., 2011). However, insertional mutagenesis remains a risk, even with such a rare integrating vector system; therefore, comprehensive genome-wide analysis of integration frequency and pattern of integrating and rare integrating vector systems in the target cell-type remains a requirement. The frequency of IDLV vectors to integrate as well as the integration pattern of ICLV vectors in human VSMCs is current unknown. This study addresses whether IDLV gene transfer of Nogo-B can mediate overexpression in VSMCs to induce phenotypic effects associated with a reduced risk of genotoxicity.

Materials and Methods

Materials

Human saphenous vein segments were obtained from patients, who gave informed consent, undergoing coronary artery bypass grafting. Ethical permission was obtained from the West Glasgow Ethics Committee (reference number: 06/S0703/110). Reagents were purchased from Sigma-Aldrich (Poole, United Kingdom) and tissue culture reagents from Gibco (Invitrogen, Paisley, United Kingdom), unless otherwise stated. All primers and probes (oligonucleotides) were obtained from MWG-Biotech (Ederberg, Germany). Nuclease-free water (not diethyl pyrocarbonate–treated) was purchased

from Ambion (Applied-Biosystems/Ambion, Warrington, United Kingdom).

Plasmids

We used the lentiviral construct plasmid encoding the marker gene, enhanced green fluorescent protein (eGFP), (pHR'SIN-cPPT-SFFV-eGFP-WPRE) under the control of the spleen focus forming virus (SFFV) promoter, as published previously (Demaison *et al.,* 2002). Nogo-B complementary DNA (haemagglutinin tagged) (Acevedo *et al.,* 2004) was cloned into the lentiviral construct plasmid containing a multiple cloning site (MCS) (pHR'SIN-cPPT-SFFV-MCS-WPRE) (Ward *et al.,* 2011) using *BamHI* and *XhoI* sites. All LVs were pseudotyped with the vesicular stomatitis virus glycoprotein (VSV-g) expressed by the pMD.G2 plasmid, as previously described (Demaison *et al.,* 2002). The second-generation LV packaging plasmid containing either the wild-type integrase gene (pCMV delta R8.74) or integrase-deficient gene (pCMV delta R8.74 D64V) was used, as detailed elsewhere (Yanez-Munoz *et al.,* 2006).

Lentiviral production and titre assay

Self-inactivating (SIN) HIV-1–based LVs were produced using a three-plasmid transient transfection system and concentrated by ultracentrifugation at 90353 × g (23,000 rpm) for 1 hr and 7 min at 4°C using a Beckmann ultracentrifuge, as previously described (Demaison *et al.,* 2002; Buckley *et al.,* 2008). LV stocks were titrated by infecting 293T cells (ATCC-LGC Standards, Middlesex, United Kingdom) with serial dilutions of LVs (Demaison *et al.,* 2002). We quantified LV genomic copy number in DNA extracted from 293T cells, 3 days post-infection, by TaqMan quantitative polymerase chain reaction (PCR), as previously described, according to a published protocol for late reverse transcriptase amplicon quantification (Butler *et al.,* 2001), and standard curves were generated using LV construct plasmid DNA as described (Butler *et al.,* 2001). LV titres were calculated as infectious viral units per ml (iu/ml).

SMC isolation, SMC culturing, and lentiviral transduction

VSMCs were isolated from human saphenous vein segments using the explant technique (Southgate and Newby, 1990) and cultured in smooth muscle cell (SMC) growth media 2 (PromoCell, Heidelberg, Germany) with the addition of the supplement mix, plus 10% (v/v) fetal calf serum (FCS) (for a 15% (v/v) FCS final concentration), 1% (v/v) penicillin, 100 μg/ml streptomycin, and 2 m*M* L-glutamine (15% complete SMC media). Passages 3–8 were used for experiments. Ad5-expressing haemagglutinin (HA)-tagged full-length human Nogo-B (Ad-Nogo-B) was generated as previously described (Acevedo *et al.,* 2004; Kritz *et al.,* 2008) and Ad5 expressing eGFP (Ad-eGFP) was obtained from Crucell (Crucell, The Netherlands). A multiplicity of infection (MOI) per cell of LV or Ad was calculated on the basis of infective titres, iu/ml for LVs and plaque forming units per ml (pfu/ml) for Ad, and an accurate cell count before infection. Equivalent "amounts" were used for ICLVs and IDLVs in relation to their TaqMan quantitative PCR titres. Cells were infected with viral vectors for 18 hr in complete SMC media, subsequently washed twice

in phosphate buffered saline (PBS), and maintained in complete SMC media. LV transductions were performed in the presence of 8 μg/ml of polybrene.

Fluorimetry and bicinchoninic acid assay

Expression of eGFP was visualized by fluorescence microscopy prior to cell lysis using 0.2% (v/v) Triton-X-100 PBS. The expression of eGFP was quantified by plate assay (fluorimetry) using a Wallac Victor 2 and recombinant eGFP (Clontech, Basingstoke, United Kingdom) as a standard, as previously described (Dishart *et al.,* 2003). Expression of eGFP was normalized to total mg of protein present (determined by a bicinchoninic acid [BCA] assay [Fisher Scientific, Loughborough, United Kingdom]), and results were expressed as relative fluorescent units (RFU)/mg protein (Dishart *et al.,* 2003).

Immunocytofluorescence

Nogo-B immunocytofluorescence in VSMCs was performed 5 days post-infection as described previously (Acevedo *et al.,* 2004; Rodriguez-Feo *et al.,* 2007; Kritz *et al.,* 2008; Yu *et al.,* 2009). Briefly, VSMCs were fixed in 4% paraformaldehyde (PFA) for 10 min, permeabilized for 10 min in 0.1% (v/v) Triton X-100 in PBS, blocked using 10% (v/v) donkey serum and 1% (w/v) BSA in PBS for 30 min, and incubated with 2 μg/ml of goat anti-human Nogo (N-18) immunoglobulin G (IgG) or isotype-matched goat IgG control in PBS containing 10% donkey serum and 1% (w/v) BSA for 18 hr at 4°C. Nogo-B staining was visualized using 4 μg/ml of Alexa-Fluor 555 donkey anti-goat IgG (Invitrogen) and mounted with Prolong-Gold anti-fade reagent with 4',6-diamidino-2-phenylindole (DAPI; Invitrogen). Micrographs were captured using a Carl Zeiss LSM 510 Meta confocal microscope at ×630 magnification, and images were digitized under constant exposure time, gain, and offset.

Migration assay

VSMC migration was assessed by a scratch-wound–mediated cell migration assay (Liang *et al.,* 2007). Briefly, VSMCs were seeded for 50 to 60% confluence into 8-well culture slides (BD Biosciences, Oxford, United Kingdom) for 16 to 18 hr prior to LV infection. Once VSMCs reached 100% confluence, a scratch was created using a sterile p200 pipette tip. VSMCs were washed twice in PBS to remove cell debris and to smooth the edge of the scratch. VSMCs were maintained in 15% complete SMC media and in the incubator at 37°C. Reference lines close to the edge of the scratch were marked and images of the scratch acquired at 0 hours and 10 hours using bright-field microscopy. After 10 hours post-wounding, VSMCs were fixed in 4% PFA and haematoxylin stained and mounted in DPX. Absolute migration was measured (μm) as farthest distance the VSMCs migrated from the wound edge (average of 10 migration distances of three independent microscope fields for each condition in triplicate) using Image Pro-Plus software (Media Cybernetics, Bethesda, Maryland).

Proliferation and apoptosis assays

For both assays, VSMCs were seeded for 30% confluence after 16 to 18 hr incubation and VSMC quiescence was

induced with serum-free media [MEM supplemented with 1% (v/v) penicillin, 100 μg/ml streptomycin, 2 mM L-glutamine, and 1mM sodium pyruvate (Sigma-Aldrich)] for 48 hr prior to LV infection with 15% complete SMC media. Proliferation was assessed using a CellTiter 96 Non-Radioactive Cell Proliferation (MTT) assay (Promega, Southampton, United Kingdom) according to manufacturer's instructions and optical density quantified using a Wallac Victor 2 at wavelength of 570 nm (Kritz *et al.,* 2008). Apoptosis was assessed using Caspase-Glo 3/7 assay (Promega) according to the manufacturer's instructions and luminescence quantified using a Wallac Victor 2. Caspase 3/7 activities for all samples were normalized to that of an equal protein amount, and the results were expressed as relative luminescence units (RLU)/mg protein.

Integration site analysis

Linear amplification-mediated (LAM)-PCR insertion site analyses, 454 pyrosequencing and bioinformatical datamining. 5'long terminal repeat (LTR)- and 3'LTR-mediated LAM-PCR analyses were performed as previously described (Schmidt *et al.,* 2007; Paruzynski *et al.,* 2010). In brief, linear PCR was performed on 1μg of DNA from ICLV- and IDLV-transduced smooth muscle cells. After magnetic capture of the biotinylated single-stranded linear PCR products second-strand DNA synthesis was performed. The resulting double-stranded fragments were digested with Tsp509I or MseI respectively, and after ligation of a linker cassette the LAM-PCR amplicons were amplified by two exponential PCR steps. The resulting LAM-PCR amplicons were further prepared for 454 pyrosequencing (GS Flx; Roche Diagnostics, Basel) as described previously (Paruzynski *et al.,* 2010). Raw LAM-PCR amplicon sequences were separated according to the introduced barcode, trimmed further, and aligned to the human genome sequence using BLAT (bioinformatics) (assembly February 2009) (Kent, 2002; Paruzynski *et al.,* 2010). The propensity of IS-forming common insertion sites (CIS) was analyzed based on previously published mathematical methods (Suzuki *et al.,* 2002; Abel *et al.,* 2007; Abel *et al.,* 2011) modified based on a new statistical comparison with a generated random data set equivalent to the actual numbers of retrieved IS (Fronza *et al.,* manuscript in preparation). Briefly, to each CIS is associated a probability value that reduce the number of false positive calls resulting from increasing numbers of total IS in the genome.

Q-PCR for vector copy number. Vector copy number estimation was performed as described previously (Paruzynski *et al.,* 2012) with modifications for calculating the relative quantification of vector copies per genome. Briefly, vector copies were amplified with LTR specific primers (SKLTR 3: AGCTTGCCTTGAGTGCTTCA; LV 2 rev: GAGTCCTGCGTCGAGAGAGC) and cell copy numbers by hEPO specific primers (hEpoR-fw: CTGCTGCCAGCTTT GAGTACAC; hEpoR-rev: GAGATGCCAGAGTCAGATA CCAC). Q-PCR was performed on the LightCycler LC480 system using the SYBRGREEN I Mix (Roche) with 30 ng of genomic DNA from ICLV- and IDLV-transduced samples 14 days post transduction. For calculating vector copy numbers relative to genome copies, the LightCycler LC480 Software (Roche) was used, and values from the ICLV- and IDLV-

transduced samples were normalized to a reference DNA obtained from a HeLa single-cell clone (D10) harboring one vector copy per genome.

Statistical analysis. All values are expressed as the mean ± SEM of triplicates and three independent experiments were performed (representative of each other). Data were tested for, and shown to exhibit, Gaussian distribution by applying the Shapiro-Wilk normality test to the data. Results were statistically analyzed using the student's unpaired t-test or one-way ANOVA for Bonferroni's multiple comparisons. Statistical significance was assigned when $p < 0.05$ (GraphPad Prism v4, La Jolla, California).
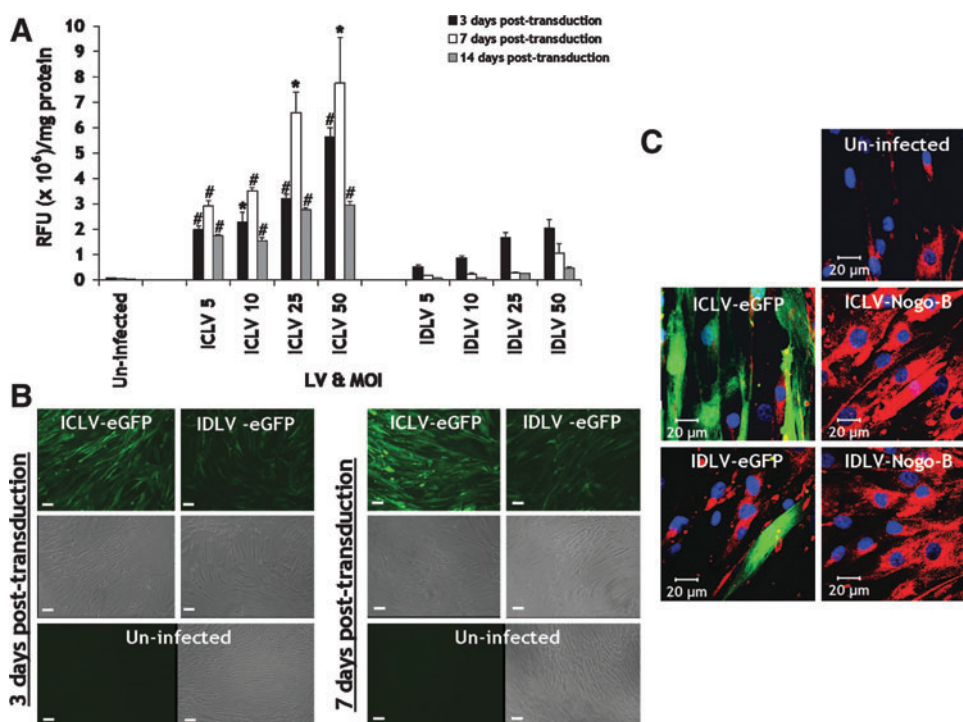
Results

IDLV-mediated gene transfer in human VSMCs

We first assessed the transduction efficiency mediated by IDLVs (IDLV-eGFP) versus their integrase-competent counterparts (ICLV-eGFP) at increasing MOIs of 5, 10, 25, and 50 in VSMCs. Expression of eGFP in VSMCs at 3, 7, and 14 days post-infection were visualized by fluorescence microscopy, prior to VSMC lysates, and quantified for eGFP expression by fluorimetry (normalized to protein). IDLV-eGFP facilitated efficient transgene expression in VSMCs, parallel to its integration-competent version (Fig. 1A). As expected, during cell division, transgene expression profiles of IDLVs decreased in a time-dependent manner from 3 days to 14 days post infection at all MOIs and mediates a bit less transgene expression than ICLV counterparts at all MOIs (Fig. 1A). Representative micrographs illustrated efficient eGFP expression in VSMCs mediated by IDLVs 3 and 7 days post infection at an MOI of 50 (Fig. 1 B). Immunocytofluorescence staining for Nogo-B indicated that both ICLV-Nogo-B and IDLV-Nogo-B mediated efficient overexpression of Nogo-B in VSMCs 5 days post-infection at an MOI of 50, compared to their eGFP configurations and endogenous Nogo-B levels observed in uninfected VSMCs (Fig. 1C). Collectively, these data support the notion that IDLVs mediate efficient gene transfer to primary human VSMCs, provide robust induction of transgene expression, and transgene expression was lost over time.

Effect of IDLV-Nogo-B on human VSMC migration

Previous reports have demonstrated that the N-terminus of Nogo-B mediates a dose-dependent inhibition of VSMC migration induced by platelet-derived growth factor-BB (PDGF-BB) (Acevedo *et al.,* 2004). We have previously shown that adenoviral overexpression of Nogo-B reduced PDGF-BB–induced migration rate of VSMCs (Kritz *et al.,* 2008). We therefore examined the effect of Nogo-B overexpression mediated by IDLV-Nogo-B on VSMC phenotypes. Migration was assessed using a scratch-wound–mediated cell migration assay and quantified 3 days post infection. A significant reduction in VSMC migration was observed after infection with IDLV-Nogo-B, compared to IDLV-eGFP, at both MOIs of 25 and 50 and uninfected VSMCs (MOI of 25: 106.24 ± 7.87 μm vs. 174.16 ± 6.49 μm [39% significant reduction in VSMC migration] or 170.15 ± 8.04 μm [38%], $p < 0.001$, respectively, and MOI of 50: 125.98 ± 8.66 μm vs. 178.9 ± 8.78 μm [30%] or 170.15 ± 8.04 μm (26%), $p < 0.001$ or $p < 0.01$, respectively) (Fig. 2A). Micrographs also illustrated IDLV-Nogo-B transduction

FIG. 1. IDLV-mediated gene transfer in VSMCs. **(A–B)** IDLVs mediated efficient eGFP expression in VSMCs. **(A)** *p < 0.01, #p < 0.001 vs. IDLV-eGFP. **(B)** Representative micrographs at an MOI of 50. Scale bar, 100 μm. **(C)** IDLV-Nogo-B (at MOI of 50) facilitated Nogo-B overexpression in VSMCs (5 days post-infection) as verified by immunocyto-fluorescence. IDLV, integrase-deficient lentiviral vectors; VSMC, vascular smooth muscle cells; eGFP, enhanced green fluorescent protein; MOI, multiplicity of infection. Color images available online at www.liebertpub.com/hum

in VSMCs inhibited migration, compared with IDLV-eGFP and untransduced VSMCs (Fig. 2B). Interestingly, our results also indicated IDLV-Nogo-B was as efficient as ICLV-Nogo-B in mediating a reduction in VSMC migration (Fig. 2A and B). Therefore, IDLV-mediated overexpression of Nogo-B attenuates VSMC migration. To note, the differences between VSMC migration at MOIs of 25 and 50 were not different in this scratch migration assay due to the sensitivity of this assay not depicting differences precisely.

IDLV-Nogo-B-mediated human VSMC proliferation

Overexpression of Nogo-B negatively regulates VSMC proliferation in response to serum and PDGF-BB stimulation, as indicated by previous studies using adenovirus-based strategies (Kritz *et al.*, 2008). We therefore investigated the effect of IDLV-Nogo-B on VSMC proliferation. IDLV-Nogo-B significantly reduced VSMC proliferation following 5 days post infection at MOIs of 25 and 50, compared to IDLV-eGFP

FIG. 2. IDLV-Nogo-B reduced VSMC migration. **(A)** IDLV-Nogo-B reduced VSMC migration, as indicated with a scratch-wound–stimulated migration of VSMCs at 3 days post infection. *p < 0.01 vs. uninfected, #p < 0.001 vs. their LV-eGFP control or uninfected. **(B)** Representative micrographs. Scale bar, 100 μm.
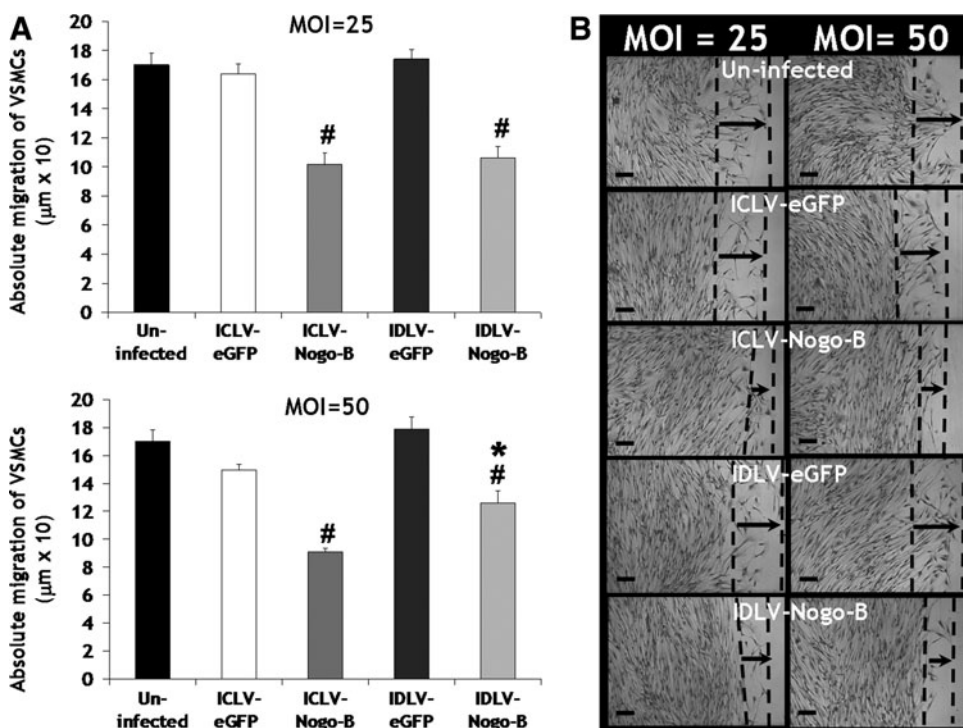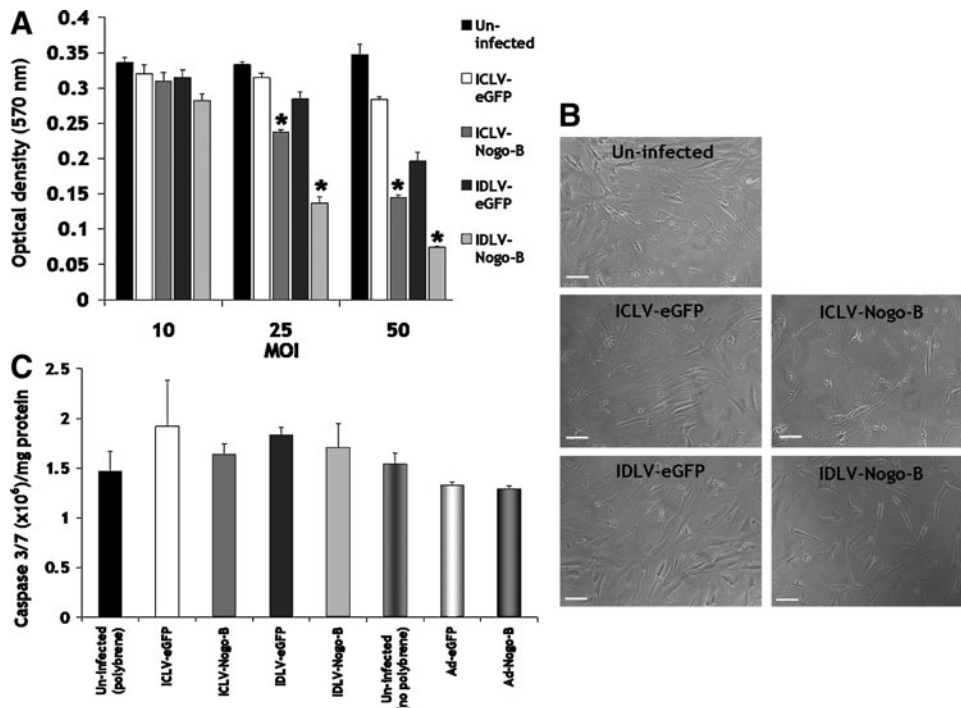
FIG. 3. IDLV-Nogo-B reduced VSMC proliferation. **(A)** IDLV-Nogo-B blocked VSMC proliferation, as assessed with an MTT assay at 5 days post infection. *p < 0.001 vs. their LV-eGFP control and uninfected. **(B)** Representative micrographs (at an MOI of 50). Scale bar, 100 μm. **(C)** IDLV-Nogo-B did not induce VSMC apoptosis, as demonstrated using a caspase-3/7 activity assay 5 days post-transduction at an MOI of 50.

control and uninfected VSMCs (MOI 25: 0.14 ± 0.0084 optical density [OD] at 570 nm vs. 0.29 ± 0.01 OD [52% significant reduction in VSMC proliferation] or 0.33 ± 0.0038 OD [58%], p < 0.001, respectively, and MOI 50: 0.074 ± 0.0011 OD vs. 0.2 ± 0.013 OD (63%) or 0.35 ± 0.015 OD [79%], p < 0.001, respectively) (Fig. 3A). Representative images are also shown at MOI of 50 (Fig. 3B). In addition, these data also demonstrated that IDLV-Nogo-B was as effective as ICLV-Nogo-B in reducing VSMC proliferation (Fig. 3A).

Previous reports have implicated that overexpression of Nogo-B can act as a pro-apoptotic protein in various cancer cells (Li *et al.,* 2001; Tambe *et al.,* 2004; Kuang *et al.,* 2006). However, we have previously reported that the overexpression of Nogo-B facilitated by adenoviral vectors in the vasculature did not induce apoptosis (Kritz *et al.,* 2008). We therefore assessed the induction of apoptosis mediated by LVs overexpressing Nogo-B in VSMCs. VSMC apoptosis was determined by a caspase-3/7 activity assay 5 days post-transduction. Results indicated that IDLV-Nogo-B and ICLV-Nogo-B at an MOI of 50 did not significantly induce casapse-3/7 activation (Fig. 3C). Therefore, IDLV-mediated elevation in Nogo-B blocks VSMC proliferation and migration in the absence of an effect on VSMC apoptosis.

Lentiviral integration site selection in human VSMCs

The above data suggests that IDLVs are effective in the context of VSMC gene transfer. Vector safety in the clinical setting is a major factor in the advancement of genetic therapies. To ascertain whether an improved safety profile of IDLV compared to ICLV could be observed in the context of vascular gene transfer, we next performed large-scale IS analyses of ICLV and IDLV vectors following infection of primary human VSMCs, and harvested DNA at 14 days post-transduction. We assessed integration by LAM-PCR and 454 pyrosequencing (Schmidt *et al.,* 2007; Gabriel *et al.,* 2009; Paruzynski *et al.,* 2010).

ICLV and IDLV vectors were used to transduce three independent human VSMC batches isolated from three different individuals at MOIs of 10, 25, and 50. Subsequent sequencing of LAM-PCR amplicons resulted in the identification of 10,752 unique ICLV IS and 1,086 multiple mappable IS sequences, mainly due to location in repetitive elements of the human

TABLE 1. OVERVIEW OF ANALYZED ICLV AND IDLV INSERTION SITES IN HUMAN VASCULAR SMOOTH MUSCLE CELLS

Patient	Vector	MOI	Unique mappable IS	Multiple mappable IS
P1	IDLV	10	20	8
		25	24	16
		50	27	18
P2	IDLV	10	16	27
		25	19	14
		50	18	11
P3	IDLV	10	24	8
		25	25	8
		50	23	8
Total			196	118
P1	ICLV	10	1972	169
		25	1475	163
		50	1950	208
P2	ICLV	10	1756	179
		25	1953	177
		50	290	40
P3	ICLV	10	778	91
		25	578	59
		50	n.d	n.d
Total			10752	1086

MOI, multiplicity of infection; IS, integration site; IDLV, integrase-deficient lentiviral vectors; ICLV, integrase-competent lentiviral vectors; n.d, no data.

genome (Table 1). IS analyses on IDLV-transduced VSMCs identified 196 unique mappable and 118 multiple mappable IS sites, clearly verifying the reduced integration frequency of IDLV-based vectors (Table 1). Strengthening the observation that most integrated IDLV genomes result from a mechanism inconsistent with residual integrase activity (see Matrai *et al.*, 2011), 28% of retrieved IDLV vector–cellular junctions contained deletions in the LTR, whereas from all ICLV insertion sites only 3% harbored deletions in the LTR. In addition, mapping of IDLV IS showed a close-to-random distribution in respect to integration within RefSeq genes (Fig. 4A). In contrast, ICLV IS showed the expected preference to integrate into RefSeq genes, independent of the different MOI used. Therefore, the sequences of the individual replicates were combined for further analyses (Fig. 4A and B).

We further analyzed the propensity of ICLV IS to be located in CIS. CIS are defined as chromosomal regions where multiple IS sites in the host genome are nonrandomly enriched. The order of CIS is defined by the number of indi-

vidual IS located in a specific genomic window size (Abel *et al.*, 2011). We did not detect any CIS while analyzing the IDLV IS; however, the analyses of the ICLV IS in patient (P)1–P3 revealed that 15 to 19% (p < 0.0001) of total IS were located in CIS of higher orders (>6th order) (Fig. 4C). Strikingly, IS in CIS were present in all three samples analyzed to a similar intensity, indicating that an intrinsic IS bias may be responsible for this observed nonrandom distribution (Fig. 4C). A total of 708 RefSeq genes were associated with these CIS, of which 24% are also listed as cancer genes (www.cbio.mskcc.org). Notably, no CIS were detected in the vicinity of *EVI1*, *MDS1*, *CCND2*, or *LMO2*, which have previously been described as genes whose insertional activation cause severe side effects in gammaretroviral gene therapy trials (Nowrouzi *et al.*, 2011). Although ICLV vectors have been shown to be intrinsically less prone to insertional mutagenesis (Montini *et al.*, 2006; Cartier *et al.*, 2009; Modlich *et al.*, 2009; Montini *et al.*, 2009; Bartholomae *et al.*, 2011; Biffi *et al.*, 2011; Nowrouzi *et al.*, 2011), this comparative analyses
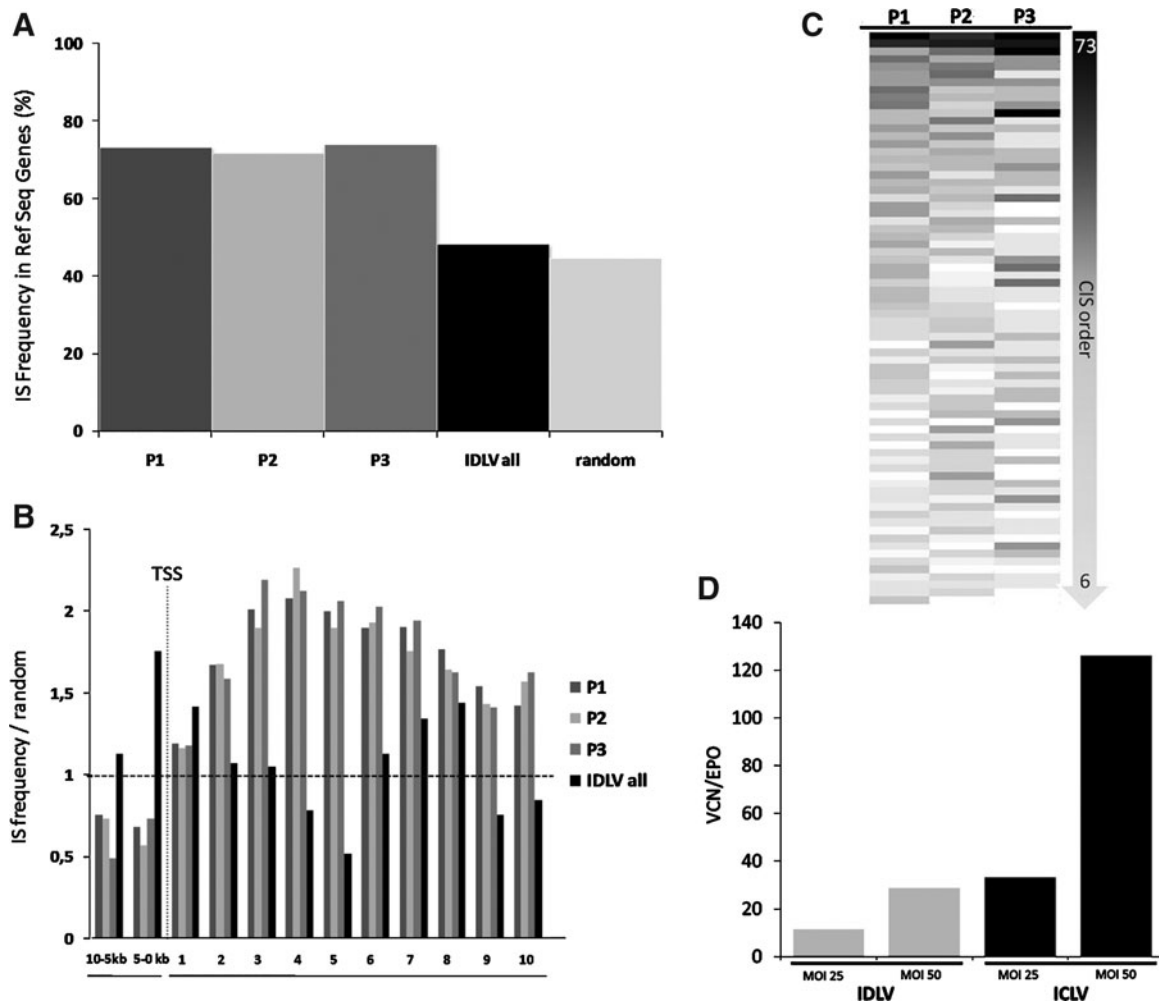

FIG. 4. Distribution of ICLV and IDLV insertion sites in human vascular smooth muscle cells. **(A)** Frequency of ICLV and IDLV integration inside RefSeq genes. **(B)** Distribution of insertion sites inside and 10 kb upstream of RefSeq genes normalized to the expected random distribution of 5.000 computer-simulated random insertion sites. **(C)** ICLV insertion sites in VSMCs show regional clustering in common insertion sites (CIS) in three independently analyzed patient samples to a similar frequency. **(D)** Vector copy number (VCN) normalized to erythropoietin (EPO) gene at 14 days post-transduction. ICLV, integrase-competent lentiviral vectors.

shows that due to the reduced integration frequency, the propensity for insertional induced deregulation of cellular genes is most likely reduced with IDLV and that IDLV-mediated gene transfer into primary human vascular cells shows a substantially improved genotoxic safety profile. For evaluating the minimal IDLV copy number required to achieve effects mediated by this particular gene delivery system in the context of vascular gene transfer, we performed q-PCR on ICLV and IDLV transduced samples 14 days post transduction (Fig. 4D). IDLV vector copy numbers (VCN) were reduced compared to ICLV 14 days post transduction (Fig. 4D). However, IDLV mediated efficient gene transfer in VSMCs (Fig. 1) and attained similar phenotypic effects compared to their integrating counterparts (Figs. 2 and 3).

Discussion

The main aim of this study was to construct and assess a suitable candidate IDLV for potential application to vascular gene therapy, and to assess the safety implications in the context of integration events in primary human vascular cells. For the first time, this study reported the important feasibility of IDLVs for use in vascular cell gene transfer studies, which provided efficient transgene expression in VSMCs and led to effective phenotypic effects on VSMC migration and proliferation *in vitro*, concomitantly associated with very low integration frequencies. Our data supports the use of IDLV in general and the potential of Nogo-B as a candidate gene for therapeutic application to acute vascular injury using this system. It has already been reported that LVs have the potential to mediate gene transfer of transgenes into primary vascular cells within a short time exposure (minutes of exposure), which is required in this clinical setting (Dishart *et al.,* 2003; Cefai *et al.,* 2005). IDLVs would be highly advantageous in vascular gene therapy based on the improved safety profile. Notably, our results here indicated efficient transgene expression in VSMCs can be achieved by IDLVs. However, IDLVs did not provide enhanced efficient and long-term eGFP expression as well as their integrase-competent counterparts in VSMCs. IDLVs expressed lower transgene expression than their integrating counterparts, which is in correlation with earlier studies (Bayer *et al.,* 2008; Matrai *et al.,* 2011).

In addition, these findings corroborated with those of previous studies in dividing cells, which reported that IDLV-mediated transient transgene expression was due to episomes lacking replication signals and thus diluting as a consequence of cell division (Nightingale *et al.,* 2006; Philippe *et al.,* 2006; Apolonia *et al.,* 2007; Matrai *et al.,* 2011). In the vascular setting *in vivo*, this is worthy of further evaluation since blockade in vascular phenotypes in the short-term post-acute injury using adenoviruses have been shown to provide long-term protection (George *et al.,* 2011). Clearly, strategies that slow or block VSMC proliferation *in vivo* would result in sustained transgene expression in the vessel wall. In addition, VSMCs have relatively low rates of proliferation in a disease state (Gordon *et al.,* 1990), and during the acute vascular injury response (Westerband *et al.,* 1997; Hilker *et al.,* 2002) with a proliferative index of approximately 1.34% (Westerband *et al.,* 1997). Therefore, it is suggested that the IDLV-mediated episomal transgene would dilute slowly, but persist for the duration required (George *et al.,* 2006; White

et al., 2007). In addition, one can speculate that Nogo-B's effect on the inhibition of VSMC proliferation would also assist with the longevity of transgene mediated by IDLV-based episomal genomes.

Previous studies have shown IDLVs, especially the D64V mutants, to have important implications relevant for gene delivery into nondividing cells within different organs (eye, muscle, central nervous system, and liver of rodents), by retaining transduction efficiency of their wild-type integrase versions with minimal host genome integration *in vitro* and *in vivo* (Yanez-Munoz *et al.,* 2006; Apolonia *et al.,* 2007; Rahim *et al.,* 2009; Matrai *et al.,* 2011). In relation to these preclinical reports, results from this *in vitro* study implied efficient gene transfer and transgene expression mediated by IDLV-Nogo-B in human VSMCs, and as consequence was as efficient in modulating phenotypic effects of VSMCs. Therefore, the data reported herein denotes the use of IDLVs as an alternative and promising gene transfer vector system. However, the lack of ability to produce the high titres for LVs (Matrai *et al.,* 2010) required for *in vivo* vascular gene transfer provides a substantial barrier and disadvantage for this vector system to be used in further vasculature studies *in vivo* at present.

We demonstrate that IS selection of ICLV in human VSMCs follows typical lentiviral target site patterns; however, regional hotspots resulting in higher order CIS have been detected. The propensity of ICLV insertions to be located in such CIS is significantly higher than expected by chance. Given that most genotoxic side effects in gene therapy trials using gammaretroviral vectors have been triggered by insertional activation of cellular genes located in close proximity to gammaretroviral CIS, it has recently been suggested that LV hotspots reflect a benign integration bias rather than oncogenic selection (Biffi *et al.,* 2011). We further show that IDLV-based vectors integrate at very low frequency and randomly in human VSMCs, and therefore reduce the risk of insertional mutagenesis. This finding is consistent with a previous report (Matrai *et al.,* 2011) and further strengthened by q-PCR, where we observed no major differences regarding VCN between IDLV (MOI of 50) and ICLV (MOI of 25). However, with LAM-PCR, we retrieved much higher integrated vector copies supporting the observed reduced integration frequency despite possible competition of episomal persisting IDLV (Fig. 4A, B, and D; Table 1).

We conclude that IDLV provide differences in VCN compared to ICLV but still attain similar phenotypic effects. In relation to these IS results, active transcriptional units of nondividing cells possess fewer LV-mediated integration frequencies, with a similar association to a random distribution of integration, unlike that of rapidly dividing cells. Moreover, LV-mediated integration sites were most commonly found in nonexpressed genes of postmitotic cells (Bartholomae *et al.,* 2011). This could have possible implications in LV-transduced VSMCs (Gordon *et al.,* 1990; Westerband *et al.,* 1997; Hilker *et al.,* 2002).

We note that IS patterns obtained from dividing VSMCs *in vitro* may not reflect the pattern of integration mediated by ICLV in VSMCs *in vivo* as described in other tissues previously (Bartholomae *et al.,* 2011). In a recent study, IDLV-mediated gene delivery in hepatocytes gave rise to random integrations without obvious skewing toward gene-coding

regions (Matrai *et al.*, 2011). Therefore, it is possible that ICLVs and most importantly IDLVs could give rise to a lesser likelihood of genotoxicity in VSMCs (Bartholomae *et al.*, 2011; Matrai *et al.*, 2011).

Taken together, this study addresses the potential of IDLVs for future use in vascular cell gene delivery studies with associated low-integration frequencies, with justification to take forward this new candidate IDLV-Nogo-B into *in vivo* models of acute vascular injury.

Acknowledgments

Author Disclosure Statement

Authors declare no conflict of interest.

References

Abbink, P., Lemckert, A.A., Ewald, B.A., *et al.* (2007). Comparative seroprevalence and immunogenicity of six rare serotype recombinant adenovirus vaccine vectors from subgroups B and D. J Virol 81, 4654–4663.

Abel, U., Deichmann, A., Bartholomae, C., *et al.* (2007). Real-time definition of non-randomness in the distribution of genomic events. PLoS One 2, e570.

Abel, U., Deichmann, A., Nowrouzi, A., *et al.* (2011). Analyzing the number of common integration sites of viral vectors - new methods and computer programs. PLoS One 6, e24247.

Acevedo, L., Yu, J., Erdjument-Bromage, H., *et al.* (2004). A new role for Nogo as a regulator of vascular remodeling. Nat Med 10, 382–388.

Apolonia, L., Waddington, S.N., Fernandes, C., *et al.* (2007). Stable gene transfer to muscle using non-integrating lentiviral vectors. Mol Ther 15, 1947–1954.

Balaggan, K.S., Duran, Y., Georgiadis, A., *et al.* (2011). Absence of ocular malignant transformation after sub-retinal delivery of rAAV2/2 or integrating lentiviral vectors in p53-deficient mice. Gene Ther 19, 182–188, 2012.

Bartholomae, C.C., Arens, A., Balaggan, K.S., *et al.* (2011). Lentiviral vector integration profiles differ in rodent postmitotic tissues. Mol Ther 19, 703–710.

Bayer, M., Kantor, B., Cockrell, A., *et al.* (2008). A large U3 deletion causes increased in vivo expression from a non-integrating lentiviral vector. Mol Ther 16, 1968–1976.

Biasco, L., Ambrosi, A., Pellin, D., *et al.* (2011). Integration profile of retroviral vector in gene therapy treated patients is cell-specific according to gene expression and chromatin conformation of target cell. EMBO Mol Med 3, 89–101.

Biasco, L., Baricordi, C., and Aiuti, A. (2012). Retroviral Integrations in Gene Therapy Trials. Mol Ther 20, 709–716.

Biffi, A., Bartholomae, C.C., Cesana, D., *et al.* (2011). Lentiviral-vector common integration sites in preclinical models and a clinical trial reflect a benign integration bias and not oncogenic selection. Blood 117, 5332–5339.

Buckley, S.M., Howe, S.J., Sheard, V., *et al.* (2008). Lentiviral transduction of the murine lung provides efficient pseudotype and developmental stage-dependent cell-specific transgene expression. Gene Ther 15, 1167–1175.

Bullard, T.A., Protack, T.L., Aguilar, F., *et al.* (2008). Identification of Nogo as a novel indicator of heart failure. Physiol Genomics 32, 182–189.

Bushman, F., Lewinski, M., Ciuffi, A., *et al.* (2005). Genome-wide analysis of retroviral DNA integration. Nat Rev Microbiol 3, 848–858.

Butler, S.L., Hansen, M.S., and Bushman, F.D. (2001). A quantitative assay for HIV DNA integration in vivo. Nat Med 7, 631–634.

Cartier, N., Hacein-Bey-Abina, S., Bartholomae, C.C., *et al.* (2009). Hematopoietic stem cell gene therapy with a lentiviral vector in X-linked adrenoleukodystrophy. Science 326, 818–823.

Cefai, D., Simeoni, E., Ludunge, K.M., *et al.* (2005). Multiply attenuated, self-inactivating lentiviral vectors efficiently transduce human coronary artery cells in vitro and rat arteries in vivo. J Mol Cell Cardiol 38, 333–344.

Demaison, C., Parsley, K., Brouns, G., *et al.* (2002). High-level transduction and gene expression in hematopoietic repopulating cells using a human immunodeficiency [correction of imunodeficiency] virus type 1-based lentiviral vector containing an internal spleen focus forming virus promoter. Hum Gene Ther 13, 803–813.

Di Lorenzo, A., Manes, T.D., Davalos, A., *et al.* (2010). Endothelial Reticulon-4B (Nogo-B) regulates ICAM-1-mediated leukocyte transmigration and acute inflammation. Blood 117, 2284–2295.

Dishart, K.L., Denby, L., George, S.J., *et al.* (2003). Third-generation lentivirus vectors efficiently transduce and phenotypically modify vascular cells: implications for gene therapy. J Mol Cell Cardiol 35, 739–748.

Gabriel, R., Eckenberg, R., Paruzynski, A., *et al.* (2009). Comprehensive genomic access to vector integration in clinical gene therapy. Nat Med 15, 1431–1436.

George, S.J., Baker, A.H., Angelini, G.D., and Newby, A.C. (1998a). Gene transfer of tissue inhibitor of metalloproteinase-2 inhibits metalloproteinase activity and neointima formation in human saphenous veins. Gene Ther 5, 1552–1560.

George, S.J., Johnson, J.L., Angelini, G.D., *et al.* (1998b). Adenovirus-mediated gene transfer of the human TIMP-1 gene inhibits smooth muscle cell migration and neointimal formation in human saphenous vein. Hum Gene Ther 9, 867–877.

George S.J., Lloyd, C.T., Angelini, G.D., *et al.* (2000). Inhibition of late vein graft neointima formation in human and porcine models by adenovirus-mediated overexpression of tissue inhibitor of metalloproteinase-3. Circulation 101, 296–304.

George, S.J., Angelini, G.D., Capogrossi, M.C., and Baker, A.H. (2001). Wild-type p53 gene transfer inhibits neointima formation in human saphenous vein by modulation of smooth muscle cell migration and induction of apoptosis. Gene Ther 8, 668–676.

George, S.J., Channon, K.M., and Baker, A.H. (2006). Gene therapy and coronary artery bypass grafting: current perspectives. Curr Opin Mol Ther 8, 288–294.

George, S.J., Wan, S., Hu, J., *et al.* (2011). Sustained Reduction of Vein Graft Neointima Formation by Ex Vivo TIMP-3 Gene Therapy. Circulation 124, S135–S142.

Gordon, D., Reidy, M.A., Benditt, E.P., and Schwartz, S.M. (1990). Cell proliferation in human coronary arteries. Proc Natl Acad Sci U S A 87, 4600–4604.

Hacein-Bey-Abina, S., Von Kalle, C., Schmidt, M., *et al.* (2003a). A serious adverse event after successful gene therapy for X-linked severe combined immunodeficiency. N Engl J Med 348, 255–256.

Hacein-Bey-Abina, S., Von Kalle, C., Schmidt, M., *et al.* (2003b). LMO2-associated clonal T cell proliferation in two patients after gene therapy for SCID-X1. Science 302, 415–419.

Hacein-Bey-Abina, S., Garrigue, A., Wang, G.P., *et al.* (2008). Insertional oncogenesis in 4 patients after retrovirus-mediated gene therapy of SCID-X1. J Clin Invest 118, 3132–3142.

Hedman, M., Hartikainen, J., and Yla-Herttuala, S. (2011). Progress and prospects: hurdles to cardiovascular gene therapy clinical trials. Gene Ther 18, 743–749.

Hilker, M., Tellmann, G., Buerke, M., *et al.* (2002). Proliferative activity in stenotic human aortocoronary bypass grafts. Cardiovasc Pathol 11, 284–290.

Howe, S.J., Mansour, M.R., Schwarzwaelder, K., *et al.* (2008). Insertional mutagenesis combined with acquired somatic mutations causes leukemogenesis following gene therapy of SCID-X1 patients. J Clin Invest 118, 3143–3150.

Janssens, S., Flaherty, D., Nong, Z., *et al.* (1998). Human endothelial nitric oxide synthase gene transfer inhibits vascular smooth muscle cell proliferation and neointima formation after balloon injury in rats. Circulation 97, 1274–1281.

Johnson, T.W., Wu Y.X., Herdeg, C., *et al.* (2005). Stent-based delivery of tissue inhibitor of metalloproteinase-3 adenovirus inhibits neointimal formation in porcine coronary arteries. Arterioscler Thromb Vasc Biol 25, 754–759.

Kane, N.M., Nowrouzi, A., Mukherjee, S., *et al.* (2010). Lentivirus-mediated reprogramming of somatic cells in the absence of transgenic transcription factors. Mol Ther 18, 2139–2145.

Karvinen, H., and Yla-Herttuala, S. (2010). New aspects in vascular gene therapy. Curr Opin Pharmacol 10, 208–211.

Kent, W.J. (2002). BLAT–the BLAST-like alignment tool. Genome Res 12, 656–664.

Kibbe, M.R., Tzeng, E., Gleixner, S.L., *et al.* (2001). Adenovirus-mediated gene transfer of human inducible nitric oxide synthase in porcine vein grafts inhibits intimal hyperplasia. J Vasc Surg 34, 156–165.

Kritz, A.B., Yu, J., Wright, P.L., *et al.* (2008). In vivo modulation of Nogo-B attenuates neointima formation. Mol Ther 16, 1798–1804.

Kuang, E., Wan, Q., Li X., *et al.* (2006). ER stress triggers apoptosis induced by Nogo-B/ASY overexpression. Exp Cell Res 312, 1983–1988.

Lee, W.S., Kim, S.W., Hong, S.A., *et al.* (2009). Atherosclerotic progression attenuates the expression of Nogo-B in autopsied coronary artery: pathology and virtual histology intravascular ultrasound analysis. J Korean Med Sci 24, 596–604.

Lewinski, M.K., Yamashita, M., Emerman, M., *et al.* (2006). Retroviral DNA integration: viral and cellular determinants of target-site selection. PLoS Pathog 2, e60.

Li, Q., Qi, B., Oka, K., *et al.* (2001). Link of a new type of apoptosis-inducing gene ASY/Nogo-B to human cancer. Oncogene 20, 3929–3936.

Liang, C.C., Park, A.Y., and Guan, J.L.. (2007). In vitro scratch assay: a convenient and inexpensive method for analysis of cell migration in vitro. Nat Protoc 2, 329–333.

Marin, E.P., Moeckel, G., Al-Lamki, R., *et al.* (2010). Identification and Regulation of Reticulon 4B (Nogo-B) in Renal Tubular Epithelial Cells. Am J Pathol 177, 2765–2773.

Matrai, J., Chuah, M.K., and Vandendriessche, T. (2010). Recent advances in lentiviral vector development and applications. Mol Ther 18, 477–490.

Matrai, J., Cantore, A., Bartholomae, C.C., *et al.* (2011). Hepatocyte-targeted expression by integrase-defective lentiviral vectors induces antigen-specific tolerance in mice with low genotoxic risk. Hepatology 53, 1696–1707.

Miao, R.Q., Gao, Y., Harrison, K.D., *et al.* (2006). Identification of a receptor necessary for Nogo-B stimulated chemotaxis and

morphogenesis of endothelial cells. Proc Natl Acad Sci U S A 103, 10997–11002.

Modlich, U., Navarro, S., Zychlinski, D., *et al.* (2009). Insertional transformation of hematopoietic cells by self-inactivating lentiviral and gammaretroviral vectors. Mol Ther 17, 1919–1928.

Montini, E., Cesana, D., Schmidt, M., *et al.* (2006). Hematopoietic stem cell gene transfer in a tumor-prone mouse model uncovers low genotoxicity of lentiviral vector integration. Nat Biotechnol 24, 687–696.

Montini, E., Cesana, D., Schmidt, M., *et al.* (2009). The genotoxic potential of retroviral vectors is strongly modulated by vector design and integration site selection in a mouse model of HSC gene therapy. J Clin Invest 119, 964–975.

Munoz, J.P., and Zorzano, A. (2011). Endoplasmic reticulum stress enters a Nogo zone. Sci Transl Med 3, 88ps26.

Nicklin, S.A., Von Seggern, D.J., Work, L.M., *et al.* (2001). Ablating adenovirus type 5 fiber-CAR binding and HI loop insertion of the SIGYPLP peptide generate an endothelial cell-selective adenovirus. Mol Ther 4, 534–542.

Nightingale, S.J., Hollis, R.P., Pepper, K.A., *et al.* (2006). Transient gene expression by nonintegrating lentiviral vectors. Mol Ther 13, 1121–1132.

Nowrouzi, A., Glimm, H., Von Kalle, C., and Schmidt, M. (2011). Retroviral Vectors: Post-Entry Events and Genomic Alterations. Viruses 3, 429–455.

Oertle, T., and Schwab, M.E. (2003). Nogo and its paRTNers. Trends Cell Biol 13, 187–194.

Oertle, T., Merkler, D., and Schwab, M.E. (2003). Do cancer cells die because of Nogo-B? Oncogene 22, 1390–1399.

Pan, J.W., Wie, M., Yang, P.Y., *et al.* (2007). Regulation of Nogo-B expression in the lesion of aortic aneurysms. Clin Exp Pharmacol Physiol 34, 856–860.

Parker, A.L., Waddington, S.N., Buckley, S.M., *et al.* (2009). Effect of neutralizing sera on factor x-mediated adenovirus serotype 5 gene transfer. J Virol 83, 479–483.

Paruzynski, A., Arens, A., Gabriel, R., *et al.* (2010). Genome-wide high-throughput integrome analyses by nrLAM-PCR and next-generation sequencing. Nat Protoc 5, 1379–1395.

Paruzynski, A., Glimm, H., Schmidt, M., and Kalle, C. (2012). Analysis of the clonal repertoire of gene-corrected cells in gene therapy. Methods Enzymol 507, 59–87.

Paszkowiak, J.J., Maloney, S.P., Kudo, F.A., *et al.* (2007). Evidence supporting changes in Nogo-B levels as a marker of neointimal expansion but not adaptive arterial remodeling. Vascul Pharmacol 46, 293–301.

Philippe, S., Sarkis, C., Barkats, M., *et al.* (2006). Lentiviral vectors with a defective integrase allow efficient and sustained transgene expression in vitro and in vivo. Proc Natl Acad Sci U S A 103, 17684–17689.

Qian, Z., Haessler, M., Lemos, J.A., *et al.* (2006). Targeting vascular injury using Hantavirus-pseudotyped lentiviral vectors. Mol Ther 13, 694–704.

Rahim, A.A., Wong, A.M., Howe, S.J., *et al.* (2009). Efficient gene delivery to the adult and fetal CNS using pseudotyped nonintegrating lentiviral vectors. Gene Ther 16, 509–520.

Rissanen, T.T., and Yla-Herttuala, S. (2007). Current status of cardiovascular gene therapy. Mol Ther 15, 1233–1247.

Rodriguez-Feo, J.A., Hellings, W.E., Verhoeven, B.A., *et al.* (2007). Low levels of Nogo-B in human carotid atherosclerotic plaques are associated with an atheromatous phenotype, restenosis, and stenosis severity. Arterioscler Thromb Vasc Biol 27, 1354–1360.

Schmidt, M., Schwarzwaelder, K., Bartholomae, C., et al. (2007). High-resolution insertion-site analysis by linear amplification-mediated PCR (LAM-PCR). Nat Methods 4, 1051–1057.

Sharif, F., Hynes, S.O., Cooney, R., , et al. (2008). Gene-eluting stents: adenovirus-mediated delivery of eNOS to the blood vessel wall accelerates re-endothelialization and inhibits restenosis. Mol Ther 16, 1674–1680.

Southgate, K., and Newby, A.C. (1990). Serum-induced proliferation of rabbit aortic smooth muscle cells from the contractile state is inhibited by 8-Br-cAMP but not 8-Br-cGMP. Atherosclerosis 82, 113–123.

Sutendra, G., Dromparis, P., Wright, P., et al. (2011). The role of Nogo and the mitochondria-endoplasmic reticulum unit in pulmonary hypertension. Sci Transl Med 3, 88ra55.

Suzuki, T., Shen, H., Akagi, K., et al. (2002). New genes involved in cancer identified by retroviral tagging. Nat Genet 32, 166–174.

Tagami, S., Eguchi, Y., Kinoshita, M., et al. (2000). A novel protein, RTN-XS, interacts with both Bcl-XL and Bcl-2 on endoplasmic reticulum and reduces their anti-apoptotic activity. Oncogene 19, 5736–5746.

Tambe, Y., Isono, T., Haraguchi, S., et al. (2004). A novel apoptotic pathway induced by the drs tumor suppressor gene. Oncogene 23, 2977–2987.

Teng, F.Y., and Tang, B.L. (2008). Cell autonomous function of Nogo and reticulons: The emerging story at the endoplasmic reticulum. J Cell Physiol 216, 303–308.

Varenne, O., Pislaru, S., Gillijns, H., et al. (1998). Local adenovirus-mediated transfer of human endothelial nitric oxide synthase reduces luminal narrowing after coronary angioplasty in pigs. Circulation 98, 919–926.

Wanisch, K., and Yanez-Munoz, R.J. (2009). Integration-deficient lentiviral vectors: a slow coming of age. Mol Ther 17, 1316–1332.

Ward, N.J., Buckley, S.M., Waddington, S.N., et al. (2011). Codon optimization of human factor VIII cDNAs leads to high-level expression. Blood 117, 798–807.

Watari, A., and Yutsudo, M. (2003). Multi-functional gene ASY/Nogo/RTN-X/RTN4: apoptosis, tumor suppression, and inhibition of neuronal regeneration. Apoptosis 8, 5–9.

Westerband, A., Mills, J.L., Marek, J.M., et al. (1997). Immunocytochemical determination of cell type and proliferation rate in human vein graft stenoses. J Vasc Surg 25, 64–73.

White, K., Nicklin, S.A., and Baker, A.H. (2007). Novel vectors for in vivo gene delivery to vascular tissue. Expert Opin Biol Ther 7, 809–821.

Wright, P.L., Yu, J., Di, Y.P., et al. (2010). Epithelial reticulon 4B (Nogo-B) is an endogenous regulator of Th2-driven lung inflammation. J Exp Med 207, 2595–2607.

Xu, W., Hong, W., Shao, Y., et al. (2011). Nogo-B regulates migration and contraction of airway smooth muscle cells by decreasing ARPC 2/3 and increasing MYL-9 expression. Respir Res 12, 14.

Yanez-Munox, R.J., Balaggan, K.S., MacNeil, A., et al. (2006). Effective gene therapy with nonintegrating lentiviral vectors. Nat Med 12, 348–353.

Yang, J., Jiang, H., Chen, S.S., et al. (2010). Lentivirus-mediated RNAi targeting CREB binding protein attenuates neointimal formation and promotes re-endothelialization in balloon injured rat carotid artery. Cell Physiol Biochem 26, 441–448.

Yu, J., Fernandez-Hernando, C., Suarez, Y., et al. (2009). Reticulon 4B (Nogo-B) is necessary for macrophage infiltration and tissue repair. Proc Natl Acad Sci U S A 106, 17511–17516.

Zhang, D., Utsumi, T., Huang, H.C., et al. (2011). Reticulon 4B (Nogo-B) is a novel regulator of hepatic fibrosis. Hepatology 53, 1306–1315.

Zhao, B., Chun, C., Liu, Z., et al. (2010). Nogo-B receptor is essential for angiogenesis in zebrafish via Akt pathway. Blood 116, 5423–5433.

Address correspondence to:
Professor Andrew H. Baker
British Heart Foundation Glasgow
Cardiovascular Research Centre
Institute of Cardiovascular and Medical Sciences
University of Glasgow, 126 University Place
Glasgow, G12 8TA
United Kingdom

Email: andrew.h.baker@glasgow.ac.uk